A Mobile Cable-Tensioning Platform to Improve Crouch Gait in Children With Cerebral Palsy

Seongyun Cho, Kun-Do Lee, and Hyung-Soon Park, *Member, IEEE*

***Abstract*— Gait impairment represented by crouch gait is the main cause of decreases in the quality of lives of children with cerebral palsy. Various robotic rehabilitation interventions have been used to improve gait abnormalities in the sagittal plane of children with cerebral palsy, such as excessive flexion in the hip and knee joints, yet in few studies have postural improvements in the coronal plane been observed. The aim of this study was to design and validate a gait rehabilitation system using a new cable-driven mechanism applying assist in the coronal plane. We developed a mobile cable-tensioning platform that can control the magnitude and direction of the tension vector applied at the knee joints during treadmill walking, while minimizing the inertia of the worn part of the device for less obstructing the natural movement of the lower limbs. To validate the effectiveness of the proposed system, three different treadmill walking conditions were performed by four children with cerebral palsy. The experimental results showed that the system reduced hip adduction angle by an average of 4.57 ± 1.79° compared to unassisted walking. Importantly, we also observed improvements of hip joint kinematics in the sagittal plane, indicating that crouch gait can be improved by postural correction in the coronal plane. The device also improved anterior and lateral pelvic tilts during treadmill walking. The proposed cable-tensioning platform can be used as a rehabilitation system for crouch gait, and more specifically, for correcting gait posture with minimal disturbance to the voluntary movement.**

***Index Terms*— Crouch gait, cerebral palsy, hip adduction, gait rehabilitation, cable-driven mechanism, rehabilitation robotics.**

I. Introduction

CHILDREN with cerebral palsy (CP), a disorder caused by non-progressive neurologic injury to the developing brain that happens before, during, or soon after birth, commonly exhibit pathologic gait patterns [1]–[3]. Crouch gait, characterized by excessive flexion of hip, knee, and ankle, is one of the most frequent gait abnormalities [3]. Children with this gait deviation from CP show slow walking speed [4], excessive pelvic tilts and knee crossing [3], [5], and increased energy costs [6] during gait. The involuntary contractions and weakness of the lower limb muscles related to the distal joint movements have been considered as the main causes of crouched walking postures [1], [2]; therefore, many studies analyzed kinematics and kinetics of ankles and knees specifically in the sagittal plane [7], [8]. Since the distal joints and proximal joints are interconnected and mutually affect each other [9]–[12], it is worth studying on how the changes in proximal joint kinematics (e.g. hip joint) affect overall gait performance specifically in crouch gait. Additionally, hip flexor and adductor muscles mutually affect hip flexion and adduction angles [13]; therefore, analysis in the coronal plane, such as hip adduction, should be added to the sagittal plane analysis. Bell *et al.* demonstrated that the gait performance and quality of patients with CP steadily decrease as they age without proper interventions [14] and emphasized the need to provide gait rehabilitation interventions; however, few studies have considered the pathologic gait patterns in the coronal plane, such as excessive hip adduction, despite its contribution to crouch gait.

To date, there are many robotic gait rehabilitation systems applied for improving crouch gait, and most of them mainly focused on correction in the sagittal plane. The robotic gait rehabilitation systems can be categorized into two types: rigid exoskeleton type which can provide a greater amount of assistive force/torque via rigid structures [15]–[17], and cable-driven type [18], [19] which minimizes structural mass/inertia while less restricting movement. Lokomat was applied to assist knee and hip joint extension in crouch gait, and the improvement in the knee and hip joint kinematics as well as the enhanced ankle and pelvic tilt in the sagittal plane was reported [15]. Other studies developed knee joint exoskeleton that provides motorized knee extension assistance [16] and an ankle joint exoskeleton using a cable-actuated ankle pulley during overground walking [17] Both studies observed improved lower-extremity extension in the sagittal plane, and each showed enhanced leg muscle activation patterns and improved kinetics in the sagittal plane, respectively. However, some clinical studies reported that the rigid robotic structures add mass and inertia to the lower limb which can be a disturbing factor during gait training [20], [21]. In addition, the aligned rigid structure may also cause discomforts to the users with lower limb deformities which are variable over time. To minimize rigidity and mass, cable-driven type mechanisms have been developed for improving

Manuscript received July 12, 2021; revised November 20, 2021 and March 10, 2022; accepted April 6, 2022. Date of publication April 20, 2022; date of current version April 29, 2022. This work was supported by the Korea Advanced Institute of Science and Technology (KAIST) through the Global Singularity Research Program for 2021. *(Corresponding author: Hyung-Soon Park.)*

This work involved human subjects or animals in its research. Approval of all ethical and experimental procedures and protocols was granted by the Institutional Review Board of Korea Advanced Institute of Science and Technology under Application No. KH2019-113.

The authors are with the Department of Mechanical Engineering, Korea Advanced Institute of Science and Technology, Daejoen 34141, South Korea (e-mail: cho0410@kaist.ac.kr; gorden2002@kaist.ac.kr; hyungspark@kaist.ac.kr).

Digital Object Identifier 10.1109/TNSRE.2022.3167472

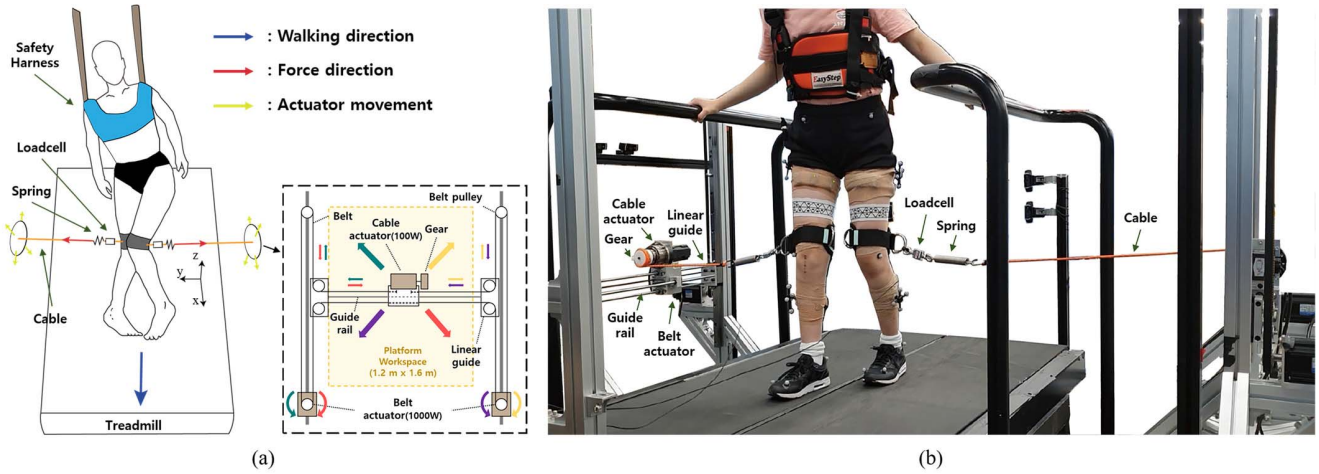

Fig. 1. Overview of a mobile tensioning platform designed to correct excessive hip adduction during gait in children with CP: (a) Schematic illustration of one participant wearing tensioned cables on both legs and a safety harness and depiction of how the platform moves parallel to the sagittal plane. (b) A subject wears knee braces that are each connected to a cable from a cable actuator over a load cell and a spring. The electromyography (EMG) measuring units below the band and reflective markers were attached to the lower limbs and pelvis.

crouch gait. Wu *et al.* demonstrated CaLT, a gait training device that attaches cables to the ankles of children with CP to apply assistance or resistance in the sagittal plane. They observed improvement in spatiotemporal gait parameters [18]. Kang *et al.* developed a cable-driven mechanism for downward pelvic pull to strengthen lower limb extensor muscles. They reported enhancement in lower limb muscle coordination and joint kinematics in the sagittal plane [19]. The major advantages of using a cable-driven mechanism for a robotic gait training system include a simple and adaptable structure for participants with different body sizes and varying deformities, and minimal addition of mass and inertia to the limbs. These are accompanied by less restriction on lower limb movement and by the active involvement of participants.

So far, the robotic interventions applied for crouch gait focused mostly on the kinematic/kinetic improvement in the sagittal plane. Previous studies analyzed the effects of the lateral movement in the lower limb on maintaining stability of body [22], [23]. Also, other studies have reported that hip joint movements in adduction/abduction direction are coupled with hip flexion/extension due to the accompanying functional roles of hip adductors and flexors [13]. In addition, hip adduction affects distal joint kinematics in crouch gait such as knee valgus and ankle eversion [9]–[12]. Thus, we hypothesized that the assistance in the coronal plane specifically targeted on the hip adduction will also contribute to improved crouch gait. In this paper, we propose a cable-driven robotic mechanism for applying assisting force in the coronal plane. In addition, we present a new cable-driven mechanism to reduce the number of cables attached to the body considering that the use of multiple cables to control both the magnitude and the direction of assisting force may restrict free movement of lower limbs since the users have to avoid collision with the cables.

In the work reported in this paper, we designed our proposed gait rehabilitation system using a cable-driven mechanism and tested the system on children with CP who exhibited excessively hip-adducted gait postures. The experiment was conducted under three conditions: (i) without device assistance, (ii) with assistance force controlled the only magnitude, and (iii) with assistance force controlled magnitude and direction by tracking the knee position. The variables that indicate gait improvement after gait training were measured and evaluated. We hypothesized that the excessive hip adduction that accompanies excessive hip joint flexion and the postural imbalance would be reduced [13], [24], and that the abnormal gait posture would be improved. Our contributions can be summarized as follows:

1) Design of a gait rehabilitation system using a cable-driven mechanism that can control the direction and magnitude of the cable tension and apply enough assistance to the lower limbs to improve gait posture

2) Use of a robust tension control algorithm that maintains the target tension of the cable attached to participants walking on a treadmill

3) Evaluation of the effectiveness of the system for individuals with CP on postural improvement in the coronal and sagittal plane

Section 2 of this paper presents the design of the cable-driven gait assisting system, details of the control algorithm, and the experimental setup and data processing. The experimental results follow in Section 3. Finally, Sections 4 and 5 close this paper with a discussion of the results and conclusions from this study, respectively.

II. Methods

This research was approved by the Institutional Review Board of Korea Advanced Institute of Science and Technology (KH2019-113, approved on 08/27/2019). Written informed consent and assent from a parent of each child were obtained prior to the experiment.

A. Mechanical System

We developed a cable tensioning system capable of providing bilateral assistance force to a participant walking on a treadmill (Fig. 1). In order to minimize the number of cables, and to control both the magnitude and the direction of net

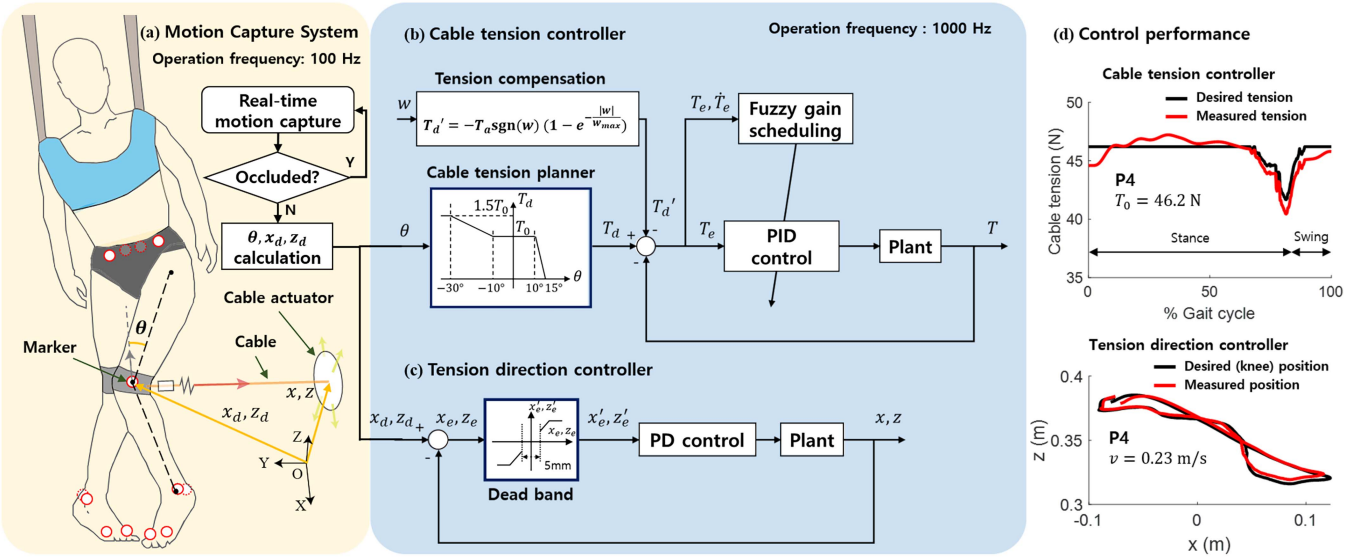

Fig. 2. Control system overview: (a) Motion capture system. (b) Cable tension controller: PID controller with the fuzzy gain scheduling for adjusting tension to correct coronal plane posture. The cable tension planner generates desired tension (T_d) based on the hip adduction angle (θ). For faster tracking of the desired tension, the tension compensator used in [17] is adopted. (c) Tension direction controller: the cable routing position in XZ plane is controlled by a PD controller to track the knee joint position in the sagittal plane. (d) Control performance: control responses of cable tension controller and tension direction controller (Example plot with P4).

assisting force, two cable actuators tracked each knee position by using a belt-driven mechanism in the two-dimensional plane (Fig. 1a). The cable actuators slide on the rails horizontally and moved vertically with the linear guides to which the rails are connected. The belt was coordinated to achieve 1.2 m × 1.6 m workspace of the cable routing position to cover possible knee locations during treadmill walking. Each participant wore only a flexible lightweight knee brace on each lower limb (Fig. 1b) to connect a cable with minimized additional mass and mechanical constraint on the lower limbs.

An actuator system on one lateral aspect comprised a 100 W servo motor (FMA-CN01, HIGEN Motor, Changwon, Republic of Korea) with a 50:1 harmonic drive strain wave gear (CSF-25B-50-J6-MSP1166, SAMICK HDS, Daegu, Republic of Korea) to apply the cable tension, a cable spool (30 mm diameter) on the gear head, and two 1000 W servo motors (FMA-CN10, HIGEN Motor, Changwon, Republic of Korea) to move the cable-tensioning platform. Each servo motor included an embedded quadrature encoder and an external servo drive (FDA-7004B, HIGEN Motor, Changwon, Republic of Korea). The two 1000 W servo motors could move a belt-driven cable actuator in a diagonal direction at the speed of up to 2.4 m/s in a 1.2 m × 1.6 m workspace parallel to the sagittal plane of participants. The cable actuator could generate a tension of up to 250 N applied to the knee brace using an inelastic cable, a spring of stiffness 2.26 N/mm, and a load cell (DBCM-50, Casscale KOREA, Seoul, Republic of Korea).

A motion capture system tracked the position of reflective markers placed on the lower limbs of participants. Eight infrared cameras (model MX, Vicon, Hauppauge, New York, USA) with an accuracy of 1 mm within a 4 m × 4 m workspace, were located around participants. The location of reflective markers on the lower limb segments and pelvis followed the Helen Hayes (HH) marker set used in previous studies and was appropriate for gait analysis [25], [26]. Nexus software (Vicon, Hauppauge, New York, USA) was used to manage and store the marker position data and for post-processing of the position trajectory.

The system control box contained a custom PCB control board that provided power and signal conditioning for the load cells and encoder quadrature and transferred signals to a DAQ card (NI-PCI-6229, National Instruments, Austin, Texas, USA) for the feedback control of servo motors with external servo drives. The system control is implemented through a custom program using Labview software (National Instruments, Austin, Texas, USA), which sends control signals to the servo motor drives to set the applied cable tension and the position of the cable actuator.

B. Control System

In the system control algorithm, the tension of the cable and the position of the cable actuator is controlled based on real-time calculation of the hip adduction angle and the knee position in the sagittal plane (Fig. 2). The feedback control system operates at 1,000 Hz (Fig. 2b), and the hip adduction angle and knee position of a participant were calculated based on the predicted hip [27] and knee [28] joint center using the reflective marker positions captured by a motion capture system at 100 Hz (Fig. 2a). When markers are occluded, tension and direction controllers use the hip adduction angle and knee position values from the previous sample step. Cable tension and the position of the cable actuator were observed using a load cell and the quadrature encoders of two belt actuators, respectively.

The cable tension controller (Fig. 2b) includes a cable tension planner, tension compensation by cable speed, and PID controller with fuzzy gain scheduling, to reduce an excessively adducted hip joint angle of each participant compared

TABLE I
PARTICIPANT INFORMATION

Participant	Age [yrs.]	Gender	Height [m]	Mass [kg]	GMFCS level	Impairment Type
Total (4)	11.3 ± 1.48	2 M / 2 F	1.42 ± 0.0941	39.8 ± 4.37	2 II / 2 III	
P1	9	M	1.30	40.4	II	Rt. Hemiplegia
P2	11	F	1.55	44.1	II	Diplegia
P3	12	F	1.37	32.6	III	Diplegia
P4	13	M	1.46	42.2	III	Quadriplegia

GMFCS: Gross Motor Function Classification System (ranges from I to IV, from the least to the most impairment, since level III participant cannot walk without a walker).

with that of a healthy person [29], [30]. The cable tension planner computes desired cable tension with respect to the hip adduction angle measured in real-time. First, within the normal ranges of hip adduction angles ($-10°$ to $10°$ from the gait kinematics of healthy children [29]), T_0 was set as the target tension value and T_0 was measured for each participant in standing to maintain 0° hip adduction. Second, outside of the normal range, the target tension was linearly interpolated by using the tension values used in the other relevant study [31]. There is the upper limb of desired tension not to disturb the patient's intended walking, experimentally set for the participant who was applied the highest reference tension. Finally, in the outside of the outer range ($-30°$ to $15°$) considering hip adduction ROM of children [30], we did not increase or decrease the target tension to avoid measurement error. Refer to the previous study about gait rehabilitation intervention using a cable-driven mechanism [19], we adopted a tension compensation algorithm to avoid a large overshoot of cable tension. The compensated tension ($T_d{}'$) was calculated using the cable actuator speed (ω) to decrease or increase the desired tension in pulling ($\omega > 0$) or pushing ($\omega < 0$) phases of an attached cable, respectively, as shown in the following equation.

$$T_d{}' = -T_a \mathrm{sgn}(\omega)[1 - \exp(-|\omega| / \omega_{\max})] \quad (1)$$

Two parameters, T_a and $\omega_{\max}$ represent maximum compensated tension and maximum cable actuator speed, respectively, and were tuned during a walking test to achieve responsive system response. Fuzzy gain scheduling scheme with proportional-integral-derivative (PID) controller was used to achieve the desired tension output with minimal error and latency [32], [33]. The gains and parameters in PID controller and fuzzy gain scheduler were tuned manually refer to the Ziegler-Nichols method and previous study about fuzzy gain scheduling [33], respectively.

The tension direction controller (Fig. 2c) that controls the origin point of the cable (x) with respect to the location of the knee (x_d) in the sagittal plane was constructed by a dead band filter and proportional-derivative (PD) control scheme. In this study, the tension direction controller controlled the origin point of the cable so that $x = x_d$ and maintain the cable perpendicular to the sagittal plane of each participant. A dead band filter that neglects input position error (x_e) less than 5 mm and more than 5 cm was applied to avoid oscillation and high acceleration caused by the sensor noise. The parameters of the dead band were determined by frequent marker position errors in the experimental environment.

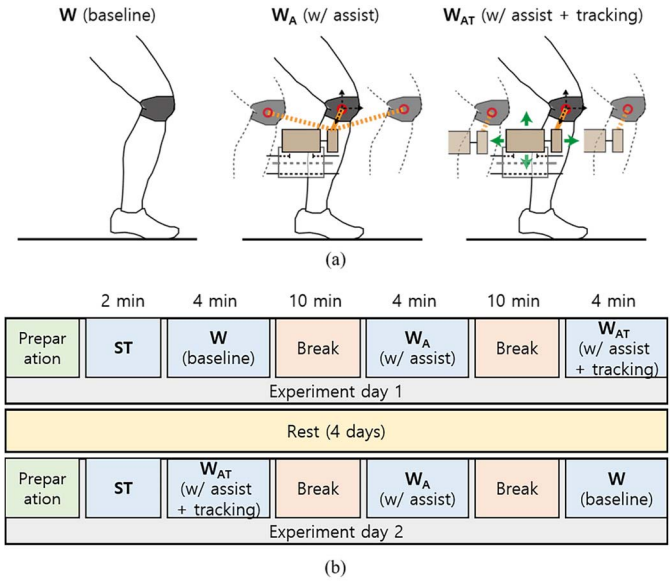

Fig. 3. (a) Schematic illustration of each walking condition. (b) Experimental protocol. ST indicates standing section for reference cable tension measurement. There was a four-day break between each experiment.

C. Recruitment

Four children with CP were recruited to participate in this study (Table I). Inclusion criteria were a diagnosis of CP, age between 6 and 18 years old, hip adducted gait posture (such as scissor gait or in-toeing with crouch gait), the ability to walk with or without a handle on a treadmill, and the cognitive ability to participate in experiments and understand simple instructions. Exclusion criteria included neurosurgery or orthopedic surgery within six months and an abnormal gait caused by developmental disorders other than CP.

D. Device Validation and Data Analysis

To validate the effectiveness of our system on children with hip adducted posture in the coronal plane by CP, each participant took part in two-day gait analysis experiments (Fig. 3). The experiment included three walking conditions

with different conditions (Fig. 3a): (i) without device assistance (W, baseline), (ii) with magnitude-controlled-assistance force without direction control by the fixed cable actuator (W_A, with assist condition), and (iii) with assistance force controlled both magnitude and direction (W_{AT}, with assist and tracking condition). In the second condition, the cable actuators were fixed at the center of a treadmill where participants initially started walking. As the participants walked on the treadmill they moved forward and backward depending on walking speed, and this caused the actuator located behind and ahead of them respectively. Each condition took four minutes in standing posture with a ten-minute break between conditions (Fig. 3b). Before the experiments, each participant was equipped with a harness, two knee braces, reflective markers, and electromyography (EMG) measuring units along with a wireless EMG system (Trigno, Delsys, Boston, Massachusetts, USA). The EMG measuring units were used to record the activation of rectus femoris (RF) with vastus lateralis (VL), biceps femoris (BF) with semitendinosus (ST), adductor longus, and lateral gastrocnemius (LG) with soleus (SL) at 1000 Hz.

Each participant completed experiments consisting of three walking conditions a day with four days of rest between experiments. The walking sessions were conducted in the condition order (i), (ii), and (iii) on the first day, and the order was reversed on the second day. To attach EMG units to the same location to measure muscle activation differences depending on the walking conditions, three walking sessions were conducted in a day. Because participants had difficulty in standing up for a long time, the preparations (attaching markers and EMG units, and measuring maximum voluntary contraction (MVC)) were carried out with participants sitting or lying down. After preparations and before the first walking condition, each reference cable tension (T_0) that corrects the hip adduction angle to 0° was measured for each participant during the standing section. Every participant wore a harness and held the handrails for safety and comfort throughout the whole experiment. No body weight support was provided for participants P1 and P2. Participants P3 and P4 (GMFCS level III) were supported 8.92 % (28.0 N) and 12.2 % (50.4 N) of body weight for static standing on the instrumented treadmill, respectively. While they walked on the treadmill, the amounts of body weight support were from a minimum of 3.18 % (9.98 N) and 7.94 % (32.7 N) to a maximum of 25.1 % (78.8 N) and 26.4 % (109 N), respectively. During gait, participants walked on a treadmill at the self-selected walking speed, but the selected speeds were not changed under different conditions. Marker trajectories and EMG data were simultaneously measured and collected by Nexus motion capture software during experiments.

A model of the skeleton of the pelvis and lower limb was constructed using a HH marker set. The model did not contain the medial aspect because of knee crossing by participants. Visual3D software (C-Motion, Inc., Gaithersburg, MD, USA) was used for the model construction and data analysis. We constructed a model using the marker data and body measurements, after which we calculated kinematic data for participants. The data were collected for 10 gait cycles, with the exception of thirty seconds at the start of each condition.

TABLE II
HEALTHY REFERENCE INFORMATION

Healthy reference	Age [years]	Gender	Height [m]	Mass [kg]
Total (21)	10.9 ± 3.17	10 M / 11 F	1.46 ± 0.207	40.8 ± 15.1
H1	10	M	1.26	24.7
H2	10	F	1.53	62.2
H3	9	F	1.35	33.0
H4	12	M	1.47	29.5

Each healthy reference subject matches participant with same number. Values are mean ± standard deviation

We analyzed EMG data from the same gait cycles used for kinematic data analysis. The EMG data were band-filtered at 20-450 Hz, notch filtered at 50 and 60 Hz, rectified, and then low-pass filtered at 10 Hz to create a linear envelope [34]. The EMG data were normalized using MVC values of each participant after filtering.

In order to compare the joint angle data of participants with unimpaired cases, we used the kinematic data during gait of gender-and-age-matched healthy children among the reference data acquired from 21 unimpaired young subjects in the previous study (Table II) [29]. The average and standard deviation of age, height, and weight of healthy and experimental (children with CP) groups were 10.9 ± 3.17 years and 11.3 ± 1.48 years, 1.46 ± 0.207 m and 1.42 ± 0.0941 m, and 40.8 ± 15.1 kg and 39.8 ± 4.37 kg, respectively.

E. Statistical Analysis

Non-parametric Friedman's test was used to analyze differences in joint kinematics and muscle activation of the more- and less-affected limbs between the three conditions using the average data across 10 gait cycles of four participants. Analysis of joint angle trajectory and muscle activation was completed separately in each single and double support at a gait cycle. Post-hoc tests were performed using Wilcoxon rank-sum tests if significant differences were detected. Data were analyzed using MATLAB software (MathWorks, Natick, Massachusetts, USA) and the statistical significances of the analysis results were $p < 0.05$. The results were expressed as mean ± standard deviation (SD).

III. RESULTS

The experimental data from three walking conditions were screened to exclude adverse events, such as toe-drag on the immovable area of a treadmill, from the kinematic data analysis. We measured the lower limb joint kinematics, muscle activities, pelvic tilt angle, and spatiotemporal gait parameters.

During the experiments, when the tensioned cables were applied, the reference tension values were 12.1 N/21.5 N, 27.2 N/30.9 N, 26.8 N/20.6 N, and 34.6 N/46.2 N for the left/right legs of P1 to P4, respectively.

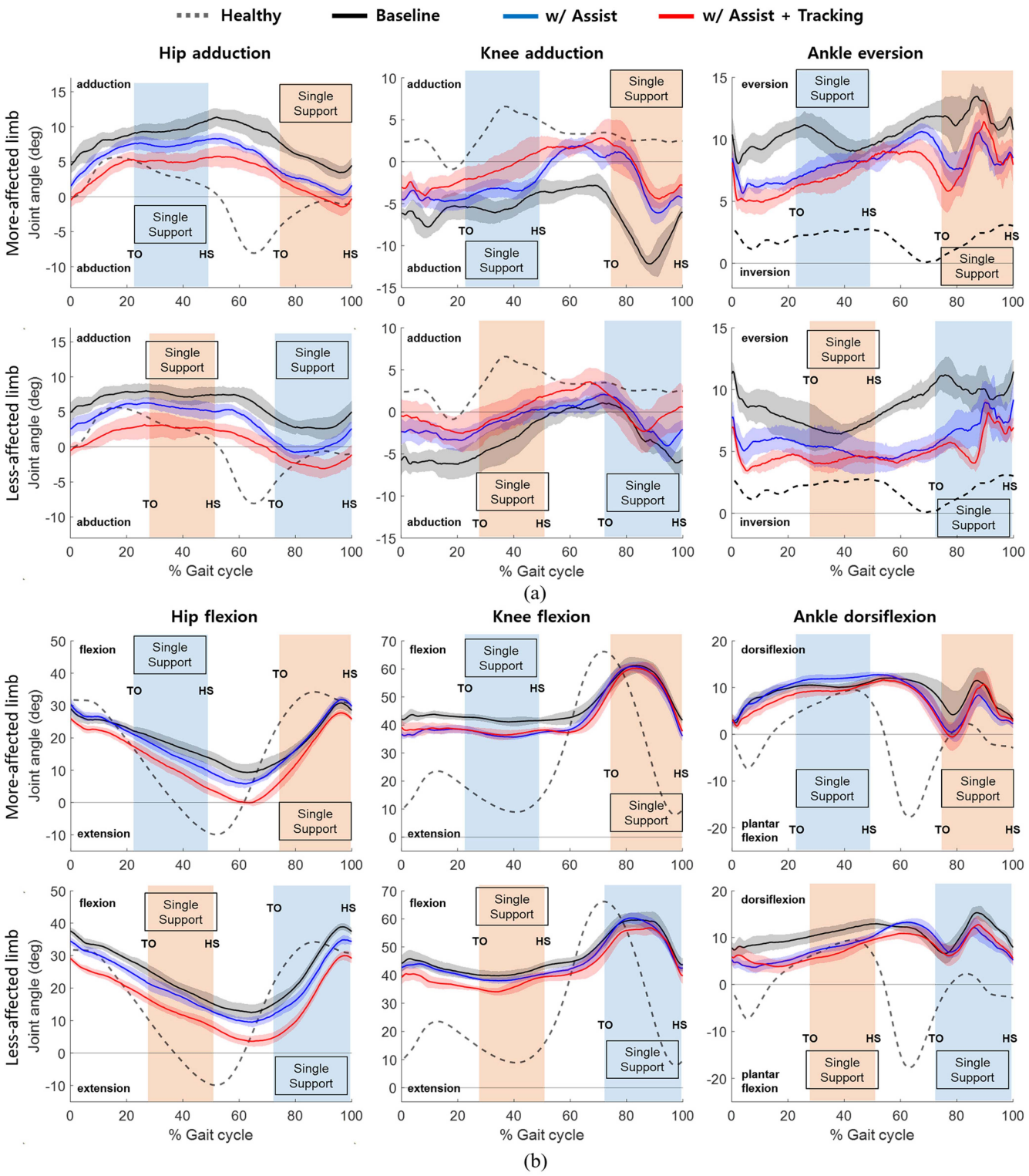

Fig. 4. Average joint angle trajectory in the (a) coronal plane and (b) sagittal plane of unimpaired references (black-dashed) and participants during baseline condition (black), with assist condition (blue), and with assist and tracking condition (red). The gait cycle starts at heel strike (HS) and ends at the next HS. A colored band represent averaged single support phase (blue: more-affected limb, orange: less-affected limb) of participants that starts at toe off (TO) and ends at HS. The shaded region represents ±1 SD from each mean.

A. Joint Kinematics

We measured lower limb joint angles during three walking conditions with and without lateral assistance applying tension through inelastic cables and springs. The reference data from unimpaired young subjects [29] of the same gender with similar age, weight, height, and leg length to each participant

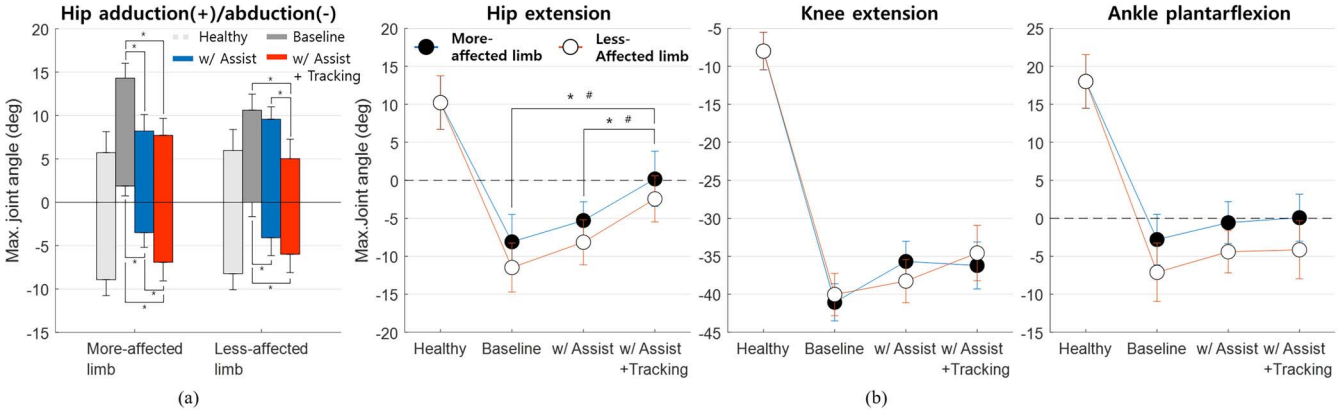

Fig. 5. Average maximum lower limb joint angles during gait. (a) Hip adduction (+) / abduction (-) angles during gait of unimpaired references (gray-dashed) and participants during baseline condition (gray), with assist condition (blue), and with assist and tracking condition (red). An asterisk (*) indicates a significant difference ($p < 0.05$) between the conditions. (b) Hip extension, knee extension, and ankle plantarflexion angles during gait of unimpaired references and participants during each condition. White and black dots represent the joint angles of less- and more-affected limbs, respectively. The symbols * and # indicate significant differences between a respective waking condition in less- and more-affected limbs, respectively ($p < 0.05$).

were compared to the measured hip adduction angle trajectory across the gait cycle.

Excessive hip adduction angles were decreased across the gait cycle with posture correction by the cable-driven mechanism using a single cable for every participant with CP (Fig. 4a). We observed the most notable reduction at each leg trajectory during the single support phase when the direction of the tension remained perpendicular to the sagittal plane of each participant (W_{AT}). For every participant, the absence of hip abduction for both legs during the gait disappeared due to the posture correction by the cable (W_A and W_{AT}).

There were also differences in the distal joint kinematics in the coronal plane. We observed increased knee adduction and decreased ankle eversion angles during assisted conditions compared to the baseline condition. The average differences across the gait cycle during W_{AT} were greater than during W_A.

Participants with crouch gait, characterized by excessively flexed hip, knee, and ankle joint, showed decreased hip flexion during walking conditions with lateral assists, W_A and W_{AT} (Fig. 4b). The greatest reduction of joint angle was also observed during W_{AT} compared to the baseline condition. There were few changes in duration of the swing and stance phase despite the differences in lower limb joint angle trajectories in every participant.

Participants walked in the excessive hip adducted postures compared to unimpaired participants in reference data, and hip abduction angles were mostly negative during free gaits without device assist (Fig. 5a). There was a $6.09 \pm 1.81°$ (more-affected, $p < 0.001$) decrease in the average maximum hip adduction angle and $5.37 \pm 1.67°$ (more-affected, $p < 0.001$) and $4.09 \pm 1.59°$ (less-affected, $p < 0.001$) increases in the average maximum hip abduction angle during W_A compared to the baseline. At the average maximum during W_{AT}, compared to the baseline, hip adduction angles decreased by $6.60 \pm 1.69°$ (more-affected, $p < 0.001$) and $5.59 \pm 2.07°$ (less-affected, $p = 0.003$) and hip abduction angles increased by $8.79 \pm 2.09°$ (more-affected, $p < 0.001$) and $5.99 \pm 1.89°$ (less-affected, $p < 0.001$). We observed a $4.54 \pm 1.84°$ (less-affected, $p = 0.010$) decrease in the average maximum hip adduction angle and a $3.42 \pm 1.92°$ (more-affected, $p = 0.021$) increase in the average maximum hip abduction angle during W_{AT} compared to W_A. In spite of the changes in the maximum hip adduction/abduction angle, the hip adduction ROM did not significantly increase for each participant by the system assist (W_A and W_{AT}).

Participants had significantly increased maximum hip extension angles of both legs, not knee and ankle joint motions in the sagittal plane, during W_{AT} compared to the other conditions ($p < 0.001$) (Fig. 5b). We observed significant increases of $8.28 \pm 3.62°$ (more-affected, $p < 0.001$) and $9.03 \pm 3.13°$ (less-affected, $p < 0.001$) at the average maximum hip extension angle of four participants during the W_{AT} compared to the baseline. The maximum hip extension angles significantly increased by $5.47 \pm 3.04°$ (more-affected, $p < 0.001$) and $5.70 \pm 3.00°$ (less-affected, $p < 0.001$) during W_{AT} compared to W_A. During W_{AT}, participants also showed positive maximum hip extension angle, which was negative for every participant during free walking, in the more-affected limb.

B. Muscle Activity

Gait posture correction using a cable-driven mechanism significantly affected the muscle activation pattern of RF in the more-affected limb (Fig. 6). Participants did not show significant differences in EMG activation of other muscles between the baseline and respective posture correction conditions (W_A and W_{AT}). We observed the average EMG of $20.2 \pm 3.03\%$, $15.5 \pm 4.25\%$, and $14.2 \pm 2.48\%$ of MVC (more-affected limb) and $21.7 \pm 3.28\%$, $19.5 \pm 3.85\%$, and $17.7 \pm 3.28\%$ of MVC (less-affected limb) in the RF for the more and less-affected limb during the baseline, W_A, and W_{AT}, respectively. In the BF, coactivated as an antagonist muscle of the RF, the average EMG values were $24.7 \pm 1.60\%$, $22.9 \pm 2.36\%$, and $23.9 \pm 2.25\%$

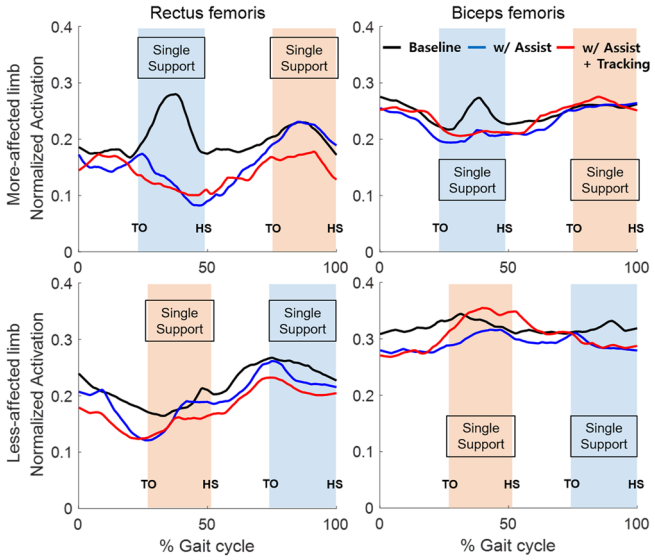

Fig. 6. Average normalized EMG (linear enveloped) of rectus femoris and biceps femoris across the gait cycle during baseline condition (black), with assist condition (blue), and with assist and tracking condition (red). A colored band represent averaged single support phase (blue: more-affected limb, orange: less-affected limb) of each participant that starts at toe off (TO) and ends at heel strike (HS).

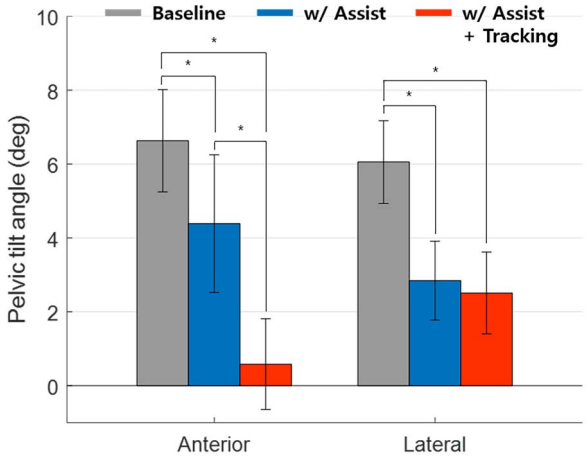

Fig. 7. Average pelvic tilt angle of participants during the baseline condition (gray), with assist condition (blue), and with assist and tracking condition (red). Lateral pelvic tilt angle is an absolute value. An asterisk (*) indicates a significant difference between respective walking conditions ($p < 0.05$).

of MVC (more-affected limb) and 32.0 ± 0.931%, 29.2 ± 1.25%, and 30.7 ± 2.73% of MVC (less-affected limb) for the more and less-affected limb during the baseline, W_A, and W_{AT}, respectively. There were significant decreases in the main knee flexor muscle (RF) activation across the gait cycle during the first single support phase ($p < 0.001$), when the maximum knee extension of the more-affected limb was observed.

C. Pelvic Tilt

We observed both decreased anterior and lateral mean pelvic tilt angles during walking conditions with posture correction (W_A and W_{AT}) (Fig. 7). There were decreases of 2.24 ± 1.62° ($p = 0.047$) in the anterior aspect and 3.21 ± 1.09° ($p < 0.001$) in the lateral aspect of the mean pelvic tilt angles during W_A compared to the baseline. During W_{AT}, compared to the baseline, the mean pelvic tilt angle decreases were 6.05 ± 1.31° ($p < 0.001$) in the anterior aspect and 3.55 ± 1.12° ($p < 0.001$) in the lateral aspect. Participants walked in significantly upright gait postures only in the anterior aspect, not the lateral aspect during W_{AT} compared to W_A. The pelvic tilt angle decreased by 3.81 ± 1.55° ($p < 0.001$) in the anterior aspect during W_{AT}.

TABLE III
SPATIOTEMPORAL GAIT PARAMETERS

	More-affected limb			Less-affected limb		
Condition	W	W_A	W_{AT}	W	W_A	W_{AT}
Step Length	0.319 ± 0.0349	0.325 ± 0.0305	0.325 ± 0.0398	0.319 ± 0.0474	0.311 ± 0.0258	0.321 ± 0.0416
Stance Duration (%)	76.1 ± 5.85	75.3 ± 3.19	74.5 ± 4.34	77.6 ± 5.49	76.3 ± 2.63	75.0 ± 4.55
Toe clearance	0.0168 ± 0.0127	0.0332 ± 0.0270	**0.0403 ± 0.0226**	0.0194 ± 0.0237	0.0256 ± 0.0116	**0.0356 ± 0.0218**
Condition	W		W_A		W_{AT}	
Step Width	0.145 ± 0.0192		0.143 ± 0.0101		0.152 ± 0.0158	
Gait Asymmetry (%)	5.33 ± 0.635		4.46 ± 0.488		5.12 ± 0.551	

Toe clearance means minimum toe clearance (MTC). Values are mean ± standard deviation. Significantly different data compared to baseline (W) condition are indicated in bold ($p < 0.05$).

D. Spatiotemporal Gait Parameter

The experimental spatiotemporal gait parameters were measured were calculated under three walking conditions (Table III). Step length, step width, and toe clearance were normalized to height. Toe clearance was measured as minimum toe clearance (MTC), the lowest vertical position of toe during the swing phase. We used the symmetry factor ratio index [35], for gait asymmetry calculation as shown in the following equation.

$$\text{GaitAsymmetry}(\%) = \left|1 - \frac{\text{leftlegstancetime}}{\text{rightlegstancetime}}\right| \times 100 \quad (2)$$

We observed significant differences only in toe clearance. There were increases of 0.0239 ± 0.0152 (more-affected, $p < 0.001$) and 0.0162 ± 0.0192 (less-affected, $p = 0.008$) during W_{AT} compared to the baseline. For other gait parameters, although there were slight changes, no significant differences were observed in other gait parameters.

IV. DISCUSSION

In this study, we presented the design and evaluation of a gait rehabilitation system using a cable-driven mechanism to correct the excessively adducted hip joint in crouch gait in children with CP. We observed the effects of the cables connected to the lateral aspects of each patient's legs during walking conditions. Our analysis shows that the newly designed system, which minimizes the number of cables and controls both the magnitude and direction of the tension of the attached cable,

is capable of improving abnormal kinematic features in the coronal plane and excessive hip flexion shown in the sagittal plane of children with CP. The important advantages of using a cable-driven mechanism were minimizing negative effects of rigid structures, which add heavy mass and inertia on the lower limbs of children, such as reduced walking speed, decreased lower limb joint ROM, and declines in timing of the gait cycle (e.g., toe-off and heel strike), during gait rehabilitation. The experimental results demonstrate decreased hip adduction angle in uniform self-selected speed without assistance to walking direction, same joint ROM, and unchanged or inclined phases in the gait cycles of participants. Specifically, the system maintained hip adduction angles within the target range measured from healthy gait, thus improving the abnormal gait posture in the coronal plane.

We observed significant improvement in hip-adducted postures of both lower limbs among children with CP. Every participant held an abduction-shifted hip adduction angle trajectory that decreased excessive hip adduction during walking conditions with system assist. Excessive hip adduction is one of the causes of instability at the pelvis during mobilization because excessive hip adduction can shift body weight towards one side [22], [36]. Assisting force to correct the hip-adducted posture also resulted in decreased hip flexion, which could be expected from the previous report on the mutual correlation between hip flexion and adduction [13]. In addition, lateral assistive force decreased excessive ankle eversion angle in the hip-adducted posture, and excessive knee abduction of dynamic knee valgus was mechanically induced by hip adduction and ankle eversion [12]. There were also improvements in toe clearance in both legs, which mean participants perform a better heel strike. These results suggest that a gait posture correction using a cable-driven mechanism that provides assistance in the coronal plane could improve crouch gait with positive effects on other lower limb joint exercises. Compared to the previous literatures on improving gait of children with CP [15]–[19], which mainly focused on the gait deviations and evaluated improvements in the sagittal plane, our study intended to assist in the coronal plane and showed the feasibility of the proposed system for gait rehabilitation. The proposed system could not improve sagittal plane knee and ankle kinematics. However, it can be combined with other gait rehabilitation devices designed for the sagittal plane assist such as knee flexion and ankle dorsiflexion to further enhance crouch gait overall.

There were significant decreases in anterior and lateral pelvic tilt angles during walking conditions with the system assist. These improvements in pelvic tilts can be considered to have been affected by improved lower limb posture because hip flexion causes the acetabulum to be less inclined and anteverted which induces anterior pelvic tilt [37], and excessive hip adduction can cause postural instability in the lateral direction and pelvic tilt [38], [39]. Hip flexion causes the acetabulum to be less inclined and anteverted, and excessive hip adduction can cause postural instability in the lateral direction which induce anterior and lateral pelvic tilt, respectively. Decreased pelvic tilt can also indicate advanced weight-bearing asymmetry, uncontrolled excessive gait perturbation by balance dysfunction, and gait energy efficiency [6], [40], [41]. Thus, this system could induce significant positive outcomes in gait rehabilitation intended to treat the complex gait abnormalities of children with CP [3].

The lower limb joint angle trajectories improved most in W_{AT}, where the direction of the cable is maintained perpendicular to the sagittal plane of participants. We also observed greater increases in the maximum hip extension and decreased pelvic tilt during gait when controlling direction also (W_{AT}), not only the magnitude of the cable tension (W_A). One possible interpretation of the improved gait posture by controlling the direction of the cable tension is a decrease of the unintended tension vector, which is parallel to the sagittal plane and caused by the position difference between the cable actuator and the knee position in the sagittal plane. The unintended tension vector can interrupt the gait, especially during the swing phase when the position difference increases. This interpretation may be supported by a larger difference in the hip adduction trajectory at each single-support phase compared to the others in the gait cycle. Interestingly, the larger difference in the hip adduction trajectory between the two conditions was also observed during the swing phase of the opposite leg. The differences during both swing phases can emphasize the importance of controlling also the direction of the cable tension to reduce unintended tension vector. Our results suggest that the use of a single cable tracking the position of the attached body part during gait would be an excellent supplement to the existing cable-driven mechanism used in gait rehabilitation.

We observed significant decreases in the activation of the more-affected limb RF muscle by posture correction. In previous studies, excessive activation of RF muscle was measured during the single support phase of crouch gait in children with CP [8], [42]. There were also decreased hip flexion angles and EMG values during the single support phase of the more-affected limb in the assisted conditions. The decreased hip flexion could be explained by decreased muscle activation in RF muscle, which induces hip flexion [13]. Thus, correction of the hip-adducted gait posture in this study resulted in significant changes in muscle activation of hip flexor, which can demonstrate the improvement of crouch gait. In addition, the biggest decrease of RF muscle activation during W_{AT} compared to the baseline may indicate that posture correction in the coronal plane with reduced unintended tension vector is also more effective for abnormal hip joint motion in the sagittal plane. However, we did not observe significant differences in the EMG signals of the other lower limb muscles, even in the antagonist muscle of RF, during gait posture correction with the new system. Future work will also focus on improvements in the abnormal muscle activation patterns of children with CP after long-term training using our gait correction system.

There is still a need to verify the effectiveness of the proposed gait rehabilitation system using a cable-driven mechanism to improve training effectiveness and motor learning with induced voluntary drive under fewer restrictions of degrees of freedom [43]–[45] and minimized additional mass and inertia [20], [21]. In this work, we were able to show in a short-term study, the potential for the proposed system

using a cable-driven mechanism that minimized the number of cables, and without using any rigid robotic structure on the limbs. We will observe the post-training results for improved motor learning of children with CP after long-term training.

The primary limitation of this study was the small number of participants used to verify the gait postural improvement by the proposed system. The study should be repeated with a larger test population and higher variability of age, height, mass, and gait impairment type or level (as indicated by the GMFCS level). Another limitation was that the gait posture correction strategy did not differ depending on the types and the levels of gait impairment of the children with CP. The hip adduction trajectory after gait correction with the system had improved, but the shape of the trajectory had changed in other participants, except in P1, who showed the mildest gait impairment. We need to modify the strategy of gait posture correction according to the hip adduction angle trajectory depending on the level of gait impairment of children with CP.

V. Conclusion

This exploratory study provides evidence that a tensioned cable pulling on each lower limb from the lateral aspects of participants can result in clinical improvements for the crouched and hip adducted gait postures in children with CP. Our design using a single-cable-driven mechanism has advantages for the control strategy that applies proper cable tension for each participant along with less restriction of movement and less mass and inertia added to the limbs. Future studies using this device should investigate the effect of longer-term training to enhance motor learning and muscle activation in a broad cohort with the proposed gait rehabilitation system based on a cable-driven mechanism.

References

[1] D. H. Sutherland and J. R. Davids, "Common gait abnormalities of the knee in cerebral palsy," *Clin. Orthopaedics Related Res.*, vol. 288, pp. 139–147, Mar. 1993.

[2] S. Gulati and V. Sondhi, "Cerebral palsy: An overview," *Indian J. Pediatr.*, vol. 85, no. 11, pp. 1006–1016, 2018.

[3] S. A. Rethlefsen, G. Blumstein, R. M. Kay, F. Dorey, and T. A. L. Wren, "Prevalence of specific gait abnormalities in children with cerebral palsy revisited: Influence of age, prior surgery, and gross motor function classification system level," *Develop. Med. Child Neurol.*, vol. 59, no. 1, pp. 79–88, Jan. 2017.

[4] R. Norlin and P. Odenrick, "Development of gait in spastic children with cerebral palsy," *J. Pediatric Orthopaedics*, vol. 6, no. 6, pp. 674–680, Nov. 1986.

[5] S. A. Rethlefsen, "Causes of intoeing gait in children with cerebral palsy," *J. Bone Joint Surgery*, vol. 88, no. 10, p. 2175, Oct. 2006.

[6] B. S. S. Rosen, C. A. Tucker, and S. C. K. Lee, "Gait energy efficiency in children with cerebral palsy," in *Proc. Int. Conf. IEEE Eng. Med. Biol. Soc.*, Aug. 2006, pp. 1220–1223.

[7] C.-J. Lin, L.-Y. Guo, F.-C. Su, Y.-L. Chou, and R.-J. Cherng, "Common abnormal kinetic patterns of the knee in gait in spastic diplegia of cerebral palsy," *Gait Posture*, vol. 11, no. 3, pp. 224–232, Jun. 2000.

[8] K. M. Steele, A. Seth, J. L. Hicks, M. S. Schwartz, and S. L. Delp, "Muscle contributions to support and progression during single-limb stance in crouch gait," *J. Biomechanics*, vol. 43, no. 11, pp. 2099–2105, Aug. 2010.

[9] X. Guan *et al.*, "Effects of ankle joint motion on pelvis-hip biomechanics and muscle activity patterns of healthy individuals in knee immobilization gait," *J. Healthcare Eng.*, vol. 2019, pp. 1–10, Oct. 2019.

[10] B. Mitchell, E. Bressel, P. J. McNair, and M. E. Bressel, "Effect of pelvic, hip, and knee position on ankle joint range of motion," *Phys. Therapy Sport*, vol. 9, no. 4, pp. 202–208, Nov. 2008.

[11] S.-P. Lee and C. M. Powers, "Individuals with diminished hip abductor muscle strength exhibit altered ankle biomechanics and neuromuscular activation during unipedal balance tasks," *Gait Posture*, vol. 39, no. 3, pp. 933–938, Mar. 2014.

[12] B. Wilczyński *et al.*, "Dynamic knee valgus in single-leg movement tasks. Potentially modifiable factors and exercise training options. a literature review," *Int. J. Environ. Res. Public Health*, vol. 17, no. 21, pp. 1–17, 2020.

[13] M. Sangeux, "Biomechanics of the hip during gait," in *The Pediatric Adolescent Hip*. Cham, Switzerland: Springer, Aug. 2019, pp. 53–71.

[14] K. J. Bell, S. Ounpuu, P. A. DeLuca, and M. J. Romness, "Natural progression of gait in children with cerebral palsy," *J. Pediatric Orthopaedics*, vol. 22, no. 5, pp. 677–682, 2002.

[15] B. Patritti *et al.*, "Enhancing robotic gait training via augmented feedback," in *Proc. Annu. Int. Conf. IEEE Eng. Med. Biol.*, vol. 10, Aug. 2010, pp. 2271–2274.

[16] Z. F. Lerner, D. L. Damiano, H.-S. Park, A. J. Gravunder, and T. C. Bulea, "A robotic exoskeleton for treatment of crouch gait in children with cerebral palsy: Design and initial application," *IEEE Trans. Neural Syst. Rehabil. Eng.*, vol. 25, no. 6, pp. 650–659, Jun. 2017.

[17] Z. F. Lerner, T. A. Harvey, and J. L. Lawson, "A battery-powered ankle exoskeleton improves gait mechanics in a feasibility study of individuals with cerebral palsy," *Ann. Biomed. Eng.*, vol. 47, no. 6, pp. 1345–1356, Jun. 2019.

[18] M. Wu, J. Kim, D. J. Gaebler-Spira, B. D. Schmit, and P. Arora, "Robotic resistance treadmill training improves locomotor function in children with cerebral palsy: A randomized controlled pilot study," *Arch. Phys. Med. Rehabil.*, vol. 98, no. 11, pp. 2126–2133, Nov. 2017.

[19] J. Kang, D. Martelli, V. Vashista, I. Martinez-Hernandez, H. Kim, and S. K. Agrawal, "Robot-driven downward pelvic pull to improve crouch gait in children with cerebral palsy," *Sci. Robot.*, vol. 2, no. 8, Jul. 2017, eaan2634.

[20] S. Rossi *et al.*, "Feasibility study of a wearable exoskeleton for children: Is the gait altered by adding masses on lower limbs?" *PLoS ONE*, vol. 8, no. 9, pp. 1–9, 2013.

[21] J. H. Meuleman *et al.*, "The effect of directional inertias added to pelvis and ankle on gait," *J. Neuroeng. Rehabil.*, vol. 10, no. 1, pp. 1–12, 2013.

[22] V. T. Inman, "Functional aspects of the abductor muscles of the hip," *J. Bone Joint Surg. Am.*, vol. 29, no. 3, pp. 607–619, 1947.

[23] A. Grimaldi, "Assessing lateral stability of the hip and pelvis," *Manual Therapy*, vol. 16, no. 1, pp. 26–32, Feb. 2011.

[24] G. Steinwender, V. Saraph, E. B. Zwick, C. Steinwender, and W. Linhart, "Hip locomotion mechanisms in cerebral palsy crouch gait," *Gait Posture*, vol. 13, no. 2, pp. 78–85, Apr. 2001.

[25] R. Baker, "Gait analysis methods in rehabilitation," *J. NeuroEng. Rehabil.*, vol. 3, pp. 1–10, Dec. 2006.

[26] T. D. Collins, S. N. Ghoussayni, D. J. Ewins, and J. A. Kent, "A six degrees-of-freedom marker set for gait analysis: Repeatability and comparison with a modified Helen Hayes set," *Gait Posture*, vol. 30, no. 2, pp. 173–180, Aug. 2009.

[27] M. E. Harrington, A. B. Zavatsky, S. E. M. Lawson, Z. Yuan, and T. N. Theologis, "Prediction of the hip joint centre in adults, children, and patients with cerebral palsy based on magnetic resonance imaging," *J. Biomech.*, vol. 40, no. 3, pp. 595–602, 2007.

[28] F. Stief, "Variations of marker sets and models for standard gait analysis," in *Handbook of Human Motion*. Cham, Switzerland: Springer, 2016.

[29] T. Lencioni, I. Carpinella, M. Rabuffetti, A. Marzegan, and M. Ferrarin, "Human kinematic, kinetic and EMG data during different walking and stair ascending and descending tasks," *Sci. Data*, vol. 6, no. 1, pp. 1–10, Dec. 2019.

[30] W. N. Sankar, C. T. Laird, and K. D. Baldwin, "Hip range of motion in children: What is the norm?" *J. Pediatric Orthopaedics*, vol. 32, no. 4, pp. 399–405, 2012.

[31] X. Jin, X. Cui, and S. K. Agrawal, "Design of a cable-driven active leg exoskeleton (C-ALEX) and gait training experiments with human subjects," in *Proc. IEEE Int. Conf. Robot. Autom. (ICRA)*, May 2015, pp. 5578–5583.

[32] T. P. Blanchett, G. C. Kember, and R. Dubay, "PID gain scheduling using fuzzy logic," *ISA Trans.*, vol. 39, no. 3, pp. 317–325, 2000.

[33] Z.-Y. Zhao, M. Tomizuka, and S. Isaka, "Fuzzy gain scheduling of PID controllers," in *Proc. 1st IEEE Conf. Control Appl.*, 1992, vol. 23, no. 5, pp. 698–703.

[34] L. Van Gestel *et al.*, "To what extent is mean EMG frequency during gait a reflection of functional muscle strength in children with cerebral palsy?" *Res. Develop. Disabilities*, vol. 33, no. 3, pp. 916–923, May 2012.

[35] K. K. Patterson, W. H. Gage, D. Brooks, S. E. Black, and W. E. McIlroy, "Evaluation of gait symmetry after stroke: A comparison of current methods and recommendations for standardization," *Gait Posture*, vol. 31, no. 2, pp. 241–246, 2010.

[36] M. Fredericson, C. L. Cookingham, A. M. Chaudhari, B. C. Dowdell, N. Oestreicher, and S. A. Sahrmann, "Hip abductor weakness in distance runners with iliotibial band syndrome," *Clin. J. Sport Med.*, vol. 10, no. 3, pp. 169–175, Jul. 2000.

[37] J. Pierrepont *et al.*, "Variation in functional pelvic tilt in patients undergoing total hip arthroplasty," *Bone Joint J.*, vol. 99-B, no. 2, pp. 184–191, Feb. 2017.

[38] G. Verheyden *et al.*, "Trunk performance after stroke and the relationship with balance, gait and functional ability," *Clin. Rehabil.*, vol. 20, no. 5, pp. 451–458, May 2006.

[39] N. Genthon *et al.*, "Posturography in patients with stroke: Estimating the percentage of body weight on each foot from a single force platform," *Stroke*, vol. 39, no. 2, pp. 489–491, 2008.

[40] G. Verheyden *et al.*, "Postural alignment is altered in people with chronic stroke and related to motor and functional performance," *J. Neurol. Phys. Therapy*, vol. 38, no. 4, pp. 239–245, 2014.

[41] S. Karthikbabu, M. Chakrapani, S. Ganesan, and R. Ellajosyula, "Relationship between pelvic alignment and weight-bearing asymmetry in community-dwelling chronic stroke survivors," *J. Neurosci. Rural Pract.*, vol. 7, no. 5, pp. S037–S040, Dec. 2016.

[42] K. M. Barr, A. L. Miller, and K. B. Chapin, "Surface electromyography does not accurately reflect rectus femoris activity during gait: Impact of speed and crouch on vasti-to-rectus crosstalk," *Gait Posture*, vol. 32, no. 3, pp. 363–368, Jul. 2010.

[43] M. Lotze, C. Braun, N. Birbaumer, S. Anders, and L. G. Cohen, "Motor learning elicited by voluntary drive," *Brain*, vol. 126, no. 4, pp. 866–872, 2003.

[44] A. Kaelin-Lang, L. Sawaki, and L. G. Cohen, "Role of voluntary drive in encoding an elementary motor memory," *J. Neurophysiol.*, vol. 93, no. 2, pp. 1099–1103, Feb. 2005.

[45] S. Khaslavskaia and T. Sinkjaer, "Motor cortex excitability following repetitive electrical stimulation of the common peroneal nerve depends on the voluntary drive," *Exp. Brain Res.*, vol. 162, no. 4, pp. 497–502, 2005.